

## Preparation of Size-controlled Copper-nanoparticle-supported Catalyst Using Rapid and Uniform Heating under Microwave Irradiation

Kojirou Fuku, Shuhei Takakura, Takashi Kamegawa, Kohsuke Mori, and Hiromi Yamashita\*

*Division of Materials and Manufacturing Science, Graduate School of Engineering,  
Osaka University, 2-1 Yamada-oka, Suita, Osaka 565-0871*

(Received March 16, 2012; CL-120230; E-mail: yamashita@mat.eng.osaka-u.ac.jp)

The size-controlled Cu nanoparticles having average particle size of 4.5, 6.3, and 7.3 nm were prepared on ZnO/SBA-15 mesoporous silica by microwave-assisted alcohol reduction in the presence of surface-modifying ligands possessing different carbon chain length such as sodium laurate (C, 12) and sodium stearate (C, 18), and the efficient hydrogenation reaction of *p*-nitrophenol to *p*-aminophenol was achieved by the Cu/ZnO/SBA-15 having Cu nanoparticles with appropriate size.

The production of valuable materials by energy-conserving processes and efficient disposal of harmful chemical wastes are highly anticipated to resolve various environmental problems such as global warming and air and/or water pollution. Metallic catalyst materials have been widely utilized to achieve these objectives, and significant efforts have recently been devoted for improving catalytic performance. In general, particle size of metallic catalyst has a large effect on the catalytic activity. In order to achieve efficient catalytic reaction, it is necessary to develop the novel technique to prepare size-controlled metallic nanoparticle catalyst tailored to catalytic reaction condition.

Above all metallic catalysts that are widely used in chemical fields, noble metals such as Rh, Pt, Pd, and Au play a very important role as beneficial catalyst metals for versatile reactions, such as hydrogenation, dehydrogenation, and oxidative decomposition.<sup>1–3</sup> However, since these noble metals are very expensive with costs gradually increasing, the development of catalyst materials exhibiting high performance with cheap base metal as alternatives of noble metal is strongly desired.

Recently, Cu-nanoparticle-supported catalysts have attracted attention because Cu nanoparticles are definitely cheap in comparison with various noble metals and possess specific and high catalytic performance for various organic synthesis reactions.<sup>4–10</sup> In particular, Cu-supported ZnO catalysts have been widely utilized for various useful reactions, such as selective hydrogenation of furfural, steam reforming of CO and methanol, reduction of carbon dioxide, and oxidation of benzene to phenol.<sup>6–10</sup> Although size-controlled Cu-nanoparticle-supported catalysts can be expected to improve catalytic activity of these useful reactions, few examples of particle-size control of Cu nanoparticles have been reported because base metals such as Cu are difficult to reduce and are easily oxidized relative to the noble metals. In particular, since Cu nanoparticles easily cause sintering and agglomeration, it is very difficult to control size of nanoparticles on catalytic supports.

Microwave (Mw)-assisted alcohol reduction using selected surface-modifying reagents has recently attracted considerable attention as a prospective preparation method of size-controlled and monodispersed metal nanoparticles because the energy-efficient Mw irradiation enables rapid and uniform heating,

which is also applicable to the simple preparation of metallic nanostructured materials.<sup>11,12</sup> However, although many studies dealing with the preparations of metal colloids and clusters have been reported, there are only a few examples on Mw-assisted synthesis of supported metal nanoparticles.<sup>13</sup>

We have previously reported on a novel method to prepare nanosized metal particles on TiO<sub>2</sub> or single-site Ti-containing mesoporous silica using Mw heating.<sup>14,15</sup> Here, we carried out preparation of size-controlled Cu nanoparticles on ZnO-supported SBA-15 mesoporous silica (Cu/ZnO/SBA-15) having high thermal and chemical stability, high surface area, and high adsorption of organic molecules by the Mw-assisted alcohol reduction using surface-modifying ligands.

SBA-15 mesoporous silica was prepared according to a previous report by sol-gel process using tetraethoxysilane (TEOS: Si(OEt)<sub>4</sub>) as a silica source and triblock copolymer P123 as a template.<sup>16</sup> The suspension of SBA-15 powder (1 g) and an aqueous solution (0.33 M, 10 cm<sup>3</sup>) of Zn(NO<sub>3</sub>)<sub>2</sub> were gradually evaporated to dryness at 313 K, and then the resultant powder was calcined at 773 K for 5 h in air, resulting in the formation of ZnO/SBA-15. The deposition of Cu precursor on ZnO/SBA-15 was performed by ion-exchange.<sup>17</sup> After the aqueous solution of ammonia was dropped into the aqueous solution of CuCl<sub>2</sub> until pH 10, the ZnO/SBA-15 (1.1 g) was suspended in this aqueous solution of [Cu(NH<sub>3</sub>)<sub>4</sub>]<sup>2+</sup> in a flask and stirred at room temperature for 2 h. After filtration and washing with distilled water, the resultant powder was dried at 343 K overnight under air, resulting in the formation of Cu<sup>2+</sup>/ZnO/SBA-15. After the Cu<sup>2+</sup>/ZnO/SBA-15 (0.3 g) was suspended in ethylene glycol (40 cm<sup>3</sup>) containing sodium laurate (Lau(C=12), 0.14 g) or sodium stearate (Stea(C=18), 0.18 g) as surface-modifying ligand of Cu, the suspension was irradiated by the microwave (500 W, 2450 ± 30 MHz, MWO-1000S, Tokyo Rikakikai Co., Ltd.) for 5 min with stirring under an Ar atmosphere. After the filtration and washing with acetone and distilled water, the resultant powder was dried at 343 K overnight under air, giving Mw-Cu/ZnO/SBA-15 (Cu:ZnO:SiO<sub>2</sub> = 5:20:75 wt %). After the Mw-Cu/ZnO/SBA-15 was calcined at 723 K for 4 h in air, the resultant powder reduced by H<sub>2</sub> (20 cm<sup>3</sup> min<sup>-1</sup>) at 473 K for 1 h, resulting in the formation of Lau(C=12)- or Stea(C=18)-Cu/ZnO/SBA-15.

Figure 1 shows UV-vis spectra and sample photograph of Mw-Cu/ZnO/SBA-15 after the Mw-assisted alcohol reduction in the presence or absence of ligand. For comparison with the Mw heating, Conv-Stea(C=18)-Cu/ZnO/SBA-15 treated by conventional heating (473 K, 5 min) in ethylene glycol was also prepared using Stea(C=18) as ligand, and the UV-vis spectrum is also shown in Figure 1. In all Mw-Cu/ZnO/SBA-15 samples prepared by the Mw-assisted alcohol reduction, absorption derived from surface plasmon resonance of Cu nanoparticles

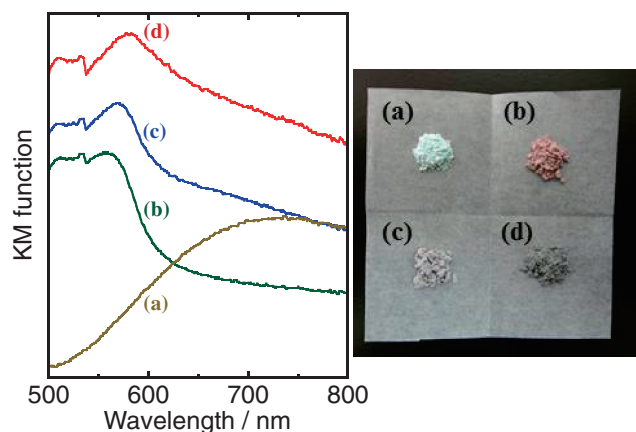


**Figure 1.** UV-vis spectra (left) and sample photograph (right) of (a) Conv-Stea(C=18)-, (b) Mw-Without ligand-, (c) Mw-Lau(C=12)-, and (d) Mw-Stea(C=18)-Cu/ZnO/SBA-15 after the Mw or conventional heating in ethylene glycol.

was observed at around 550 to 600 nm.<sup>18</sup> In addition, these samples obviously exhibited different color with the naked eye. The surface plasmon absorption of this region is observed for Cu nanoparticles larger than 5 nm.<sup>11</sup> The intensity and wavelength of the surface plasmon absorption depend on the size of Cu nanoparticles, and blue shift of this absorption region is observed with increasing size of Cu nanoparticles.<sup>18</sup> Since the remarkable tendency of blue shift was observed in the order of Stea(C=18)-, Lau(C=12)- and without ligand-Cu/ZnO/SBA-15, this result indicates that size of these Cu nanoparticles increased in the order of Stea(C=18) < Lau(C=12) < without ligand. On the other hand, the absorption derived from Cu<sup>2+</sup> at around 730 nm was obviously observed in the Conv-Stea(C=18)-Cu/ZnO/SBA-15 without surface plasmon absorption. These results suggest that Cu nanoparticles possessing different size were produced on ZnO/SBA-15 by alcohol reduction using rapid dielectric heating of the Mw.

The specific surface area ( $S_{\text{BET}}$ ) and pore volume before and after deposition of ZnO and Cu nanoparticles calculated by N<sub>2</sub> adsorption-desorption measurement are shown in Table 1. The SBA-15 mesoporous silica possesses large pore size of 7.3 nm, high  $S_{\text{BET}}$ , and pore volume, but the  $S_{\text{BET}}$  and pore volume decreased after the deposition of ZnO and Cu nanoparticles. In addition,  $S_{\text{BET}}$  and pore volume after deposition of Cu nanoparticles obviously changed by the kind of ligands and decreased in the order of without ligand > Lau(C=12) > Stea(C=18) for the blockage of pores. These results of  $S_{\text{BET}}$  and pore volume suggest that highly dispersed Cu nanoparticles were supported within the pore of SBA-15 mesoporous silica, and the order of these Cu particle size was also in close agreement with those expected from UV-vis measurement. As shown in Figure S1,<sup>19</sup> XRD patterns of various Cu/ZnO/SBA-15 also showed the same tendency because diffraction peak intensity of 43.5 and 50.5° derived from fcc structure of Cu increased in the order of Stea(C=18) < Lau(C=12) < without ligand. The obtained Cu nanoparticles were also characterized by Cu K-edge XAFS spectra (Figure 2). The XANES spectra of all samples are similar to that of Cu foil, suggesting the presence of Cu in a metallic state. In the Fourier transforms of Cu K-edge EXAFS

**Table 1.** The specific surface area ( $S_{\text{BET}}$ ) and pore volume before and after deposition of ZnO and Cu nanoparticles calculated by N<sub>2</sub> adsorption-desorption measurement

Sample	$S_{\text{BET}}$ /m <sup>2</sup> g <sup>-1</sup>	Pore volume /cm <sup>3</sup> g <sup>-1</sup>
SBA-15	677	0.94
ZnO/SBA-15	344	0.56
Without ligand	272	0.52
Lau(C=12)	249	0.51
Stea(C=18)	226	0.47

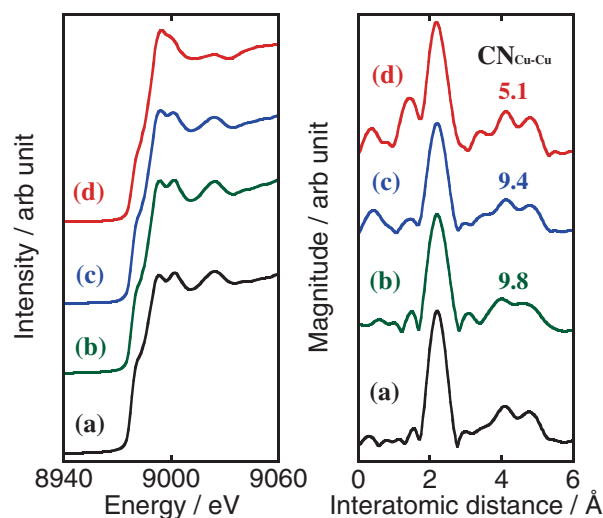


**Figure 2.** Cu K-edge XANES spectra (left) and FT-EXAFS spectra (right) of (a) Cu foil, (b) Without ligand-, (c) Lau(C=12)-, and (d) Stea(C=18)-Cu/ZnO/SBA-15.

spectra, all samples exhibited a peak at approximately 2.2 Å due to the contiguous Cu-Cu bond in the metallic form nanoparticles. In addition, the coordination number ( $\text{CN}_{\text{Cu-Cu}}$ ) of metallic Cu nanoparticles calculated by curve-fitting analysis was 5.1, 9.4, and 9.8 for Stea(C=18)-, Lau(C=12)- and without ligand-Cu/ZnO/SBA-15 respectively, as shown in Figure 2. The  $\text{CN}_{\text{Cu-Cu}}$  also increased in the order of Stea(C=18) < Lau(C=12) < without ligand, which was in close agreement with the order of the Cu particle size expected from UV-vis and N<sub>2</sub> adsorption-desorption measurement. As shown in TEM images of Figure 3, the SBA-15 mesoporous silica possessed well-ordered mesoporous channel structure, which was established from the low-angle XRD spectrum and N<sub>2</sub> adsorption-desorption measurement. Apparently, highly dispersed nano-sized Cu particles having a narrow size distribution were observed in the interior of the SBA-15 mesoporous channels. The average particle size of Cu for Stea(C=18), Lau(C=12), and without ligand was 4.5, 6.3, and 7.3 nm, respectively, and comparative results of particle size obtained by the TEM observation was consistent with those of all characterizations. These results suggest that the alcohol reduction method by Mw is one of the most promising ways to support uniform dispersion of small Cu nanoparticles on ZnO/SBA-15. The size distribution was significantly influenced by the carbon chain length of surface-modifying ligand, and longer carbon chain produced more intense aggregation inhibition effect of Cu nanoparticles.

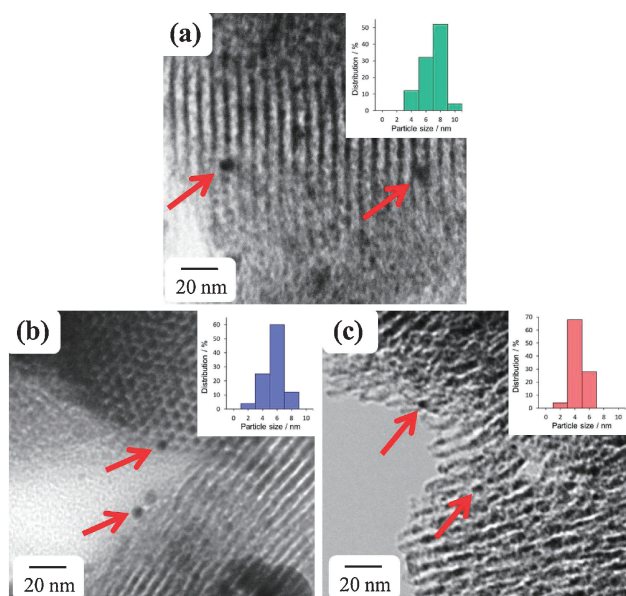


**Figure 3.** TEM images and size distribution of (a) Without ligand-, (b) Lau(C=12)-, and (c) Stea(C=18)-Cu/ZnO/SBA-15.

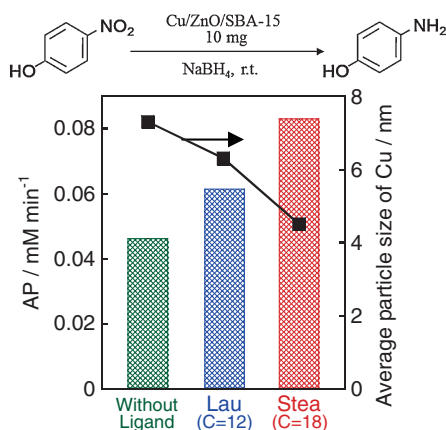


**Figure 4.** Effect of Cu particle size on the hydrogenation of NP (5 mM, 20 cm<sup>3</sup>) to AP by various Cu/ZnO/SBA-15 (10 mg) in the presence of NaBH<sub>4</sub> (3.5 equiv) under Ar.

The comparison of catalytic activity using various Cu-nanoparticle-supported ZnO/SBA-15 having different size was carried out by hydrogenation reaction of *p*-nitrophenol (NP: 5 mM, 20 cm<sup>3</sup>) to *p*-aminophenol (AP) in aqueous solution of NaBH<sub>4</sub> as reducing agent at room temperature under the Ar atmosphere. The amounts of NP and AP were measured using a UV-2450 UV-vis spectrophotometer because the NP and AP in aqueous solution containing NaBH<sub>4</sub> show maximum absorption at 400 and 300 nm, respectively (Figure S2<sup>19</sup>). As shown in Figures 4 and S2,<sup>19</sup> all Cu/ZnO/SBA-15 exhibited high hydrogenation activity of NP to AP and the NP was completely consumed within a very short time. In addition, the hydrogenation activity of NP to AP increased in the order of without ligand < Lau(C=12) < Stea(C=18). It should be noted that the order of the hydrogenation activity was in close agreement with

the order of decreasing Cu nanoparticle size. As shown in Figure S3,<sup>19</sup> the catalytic activities were almost maintained in the recycling test. These results suggest that the catalytic activity of Cu/ZnO/SBA-15 depends on the Cu nanoparticle size and that the more efficient catalytic reaction is achieved by the Cu nanoparticles with most appropriate size.

In summary, size control of Cu particle on ZnO/SBA-15 was investigated by alcohol reduction using rapid and uniform heating by Mw to achieve more efficient catalytic reaction. It was demonstrated that the Mw-assisted alcohol reduction using surface-modifying ligand possessing different carbon chain length is a promising way to dispersively support size-controlled Cu nanoparticles and these size-controlled Cu-nanoparticles-supported ZnO/SBA-15 affect the hydrogenation reaction of NP to AP.

This study was financially supported by the Grants-in-Aid for Scientific Research from the Ministry of Education, Culture, Sports, Science and Technology of Japan (No. 23360356) and the Global COE Program (Project: Center of Excellence for Advanced Structural and Function Materials Design) from the Ministry of Education, Culture, Sports, Science and Technology of Japan. The X-ray absorption experiments were performed at the photon factory of KEK.

## References and Notes

- D. A. Perry, J. C. Hemminger, *J. Am. Chem. Soc.* **2000**, *122*, 8079.
- K. Fuku, K. Hashimoto, H. Kominami, *Chem. Commun.* **2010**, *46*, 5118.
- K. Fuku, M. Goto, T. Kamegawa, K. Mori, H. Yamashita, *Bull. Chem. Soc. Jpn.* **2011**, *84*, 979.
- A. K. Patra, A. Dutta, A. Bhaumik, *Catal. Commun.* **2010**, *11*, 651.
- A. Yin, X. Guo, W.-L. Dai, K. Fan, *J. Phys. Chem. C* **2009**, *113*, 11003.
- H.-Y. Zheng, Y.-L. Zhu, Z.-Q. Bai, L. Huang, H.-W. Xiang, Y.-W. Li, *Green Chem.* **2006**, *8*, 221.
- H. Yahiro, K. Murawaki, K. Saiki, T. Yamamoto, H. Yamaura, *Catal. Today* **2007**, *126*, 436.
- Y. Matsumura, H. Ishibe, *J. Catal.* **2009**, *268*, 282.
- F. C. Meunier, *Angew. Chem., Int. Ed.* **2011**, *50*, 4053.
- I. Boz, T. G. Altınçekiç, *React. Kinet., Mech. Catal.* **2011**, *102*, 195.
- T. Nakamura, Y. Tsukahara, T. Sakata, H. Mori, Y. Kanbe, H. Bessho, Y. Wada, *Bull. Chem. Soc. Jpn.* **2007**, *80*, 224.
- M. Tsuji, M. Hashimoto, Y. Nishizawa, M. Kubokawa, T. Tsuji, *Chem.—Eur. J.* **2005**, *11*, 440.
- K. Yoshida, C. Gonzalez-Arellano, R. Luque, P. L. Gai, *Appl. Catal., A* **2010**, *379*, 38.
- K. Fuku, T. Kamegawa, K. Mori, H. Yamashita, *Chem.—Asian J.*, in press. doi:10.1002/asia.201100984.
- S. Shironita, T. Takasaki, T. Kamegawa, K. Mori, H. Yamashita, *Top. Catal.* **2010**, *53*, 218.
- K. Mori, K. Watanabe, M. Kawashima, M. Che, H. Yamashita, *J. Phys. Chem. C* **2011**, *115*, 1044.
- J. Zheng, W. Zhu, C. Ma, Y. Hou, W. Zhang, Z. Wang, *React. Kinet., Mech. Catal.* **2010**, *99*, 455.
- A. Moores, F. Goettmann, *New J. Chem.* **2006**, *30*, 1121.
- Supporting Information is available electronically on the CSJ-Journal Web site, <http://www.csj.jp/journals/chem-lett/index.html>.